Environ. Sci. Technol. **2007**, *41,* 2498−2504

Kinetic Analysis of Competition between Aerosol Particle Removal and Generation by Ionization Air Purifiers

AHMAD ALSHAWA, ASHLEY R. RUSSELL, AND SERGEY A. NIZKORODOV*

Department of Chemistry, University of California, Irvine, California 92697-2025

Ionization air purifiers are increasingly used to remove aerosol particles from indoor air. However, certain ionization air purifiers also emit ozone. Reactions between the emitted ozone and unsaturated volatile organic compounds (VOC) commonly found in indoor air produce additional respirable aerosol particles in the ultrafine (<0.1 μm) and fine (<2.5 μm) size domains. A simple kinetic model is used to analyze the competition between the removal and generation of particulate matter by ionization air purifiers under conditions of a typical residential building. This model predicts that certain widely used ionization air purifiers may actually *increase* the mass concentration of fine and ultrafine particulates in the presence of common unsaturated VOC, such as limonene contained in many household cleaning products. This prediction is supported by an explicit observation of ultrafine particle nucleation events caused by the addition of D-limonene to a ventilated office room equipped with a common ionization air purifier.

Introduction

Ultrafine (diameter <0.1 μm; $PM_{0.1}$), fine (<2.5 μm; $PM_{2.5}$), and coarse (<10 μm; PM_{10}) aerosol particles significantly contribute to the toxicity of urban air pollution (*1*, *2*). The adverse health effects of particulate matter (PM) include exacerbation of asthma symptoms (*3*, *4*), cardiovascular problems (*5*, *6*), increased mortality (*7*, *8*), and increased incidence of lung cancers (*9*, *10*). To address the health impacts of airborne PM, the Environmental Protection Agency (EPA) established the national ambient air quality standards for $PM_{2.5}$ at 15 (annual mean) and 65 $\mu g/m^3$ (24-h mean). The standards for PM_{10} are 50 and 150 $\mu g/m^3$, respectively. No official standards for ultrafine particles have been established yet in spite of the increasing evidence for their toxicity and innate ability to penetrate into the blood circulation (*11*).

A significant fraction of urban PM can be classified as secondary organic aerosol (SOA) produced by oxidation of volatile organic compounds (VOC) (*12*). A particularly important group of aerosol-forming VOC are terpenes (*13*, *14*), a class of hydrocarbons emitted by coniferous plants and used extensively as additives to many household cleaning products. The SOA yields, reaction mechanisms, and particle composition have been extensively studied for oxidation of α-pinene, β-pinene, limonene, and other monoterpenes in smog chambers under atmospherically relevant conditions (*15*−*26*) and in simulated indoor environments (*13*, *14*, *27*−*31*). The observed SOA yields resulting from oxidation by ozone can be quite high (>50% by mass), but the yields depend in a complicated way on multiple factors including presence of NO_x, presence of OH scavengers, concentration of preexisting aerosol particles, concentrations of reactants, humidity, temperature, radiation level, and reaction time.

Stand-alone air purification devices for indoor use have gained widespread popularity in recent years. However, certain air purifiers emit ozone during operation, either intentionally or as a byproduct of air ionization (*32*−*35*). Ozone, a criterion air pollutant regulated by multiple health standards, represents a serious health concern by itself (*36*). In addition, ozone can react with certain indoor surfaces (*37*−*41*) and indoor VOC (*30*, *42*−*44*) generating secondary products with potential adverse health effects. For example, terpene oxidation products are known eye and airway irritants (*45*, *46*).

Ionization air purifiers present an interesting dilemma in this respect. On one hand, they remove PM from the air. On the other hand, ozone emitted by certain ionization air purifiers in the presence of unsaturated VOC increases both the mass and number concentration of aerosol particles. The main objective of this study is to verify whether the mass emission rate of fine and ultrafine PM resulting from an ionization air purifier operation can exceed the purifier's PM removal rate under conditions characteristic of a private residence.

Experimental Section

A common residential ionization air purifier (IAP) was used in experiments. A commercial ozone generator (OG) marketed as an "air cleaner" despite its lack of any particle filtration capabilities, was used for comparison. Rates of ozone emission and particle removal (Table 1) for these two devices were quantified as described in the Supporting Information.

The measured ozone emission rates for the IAP and OG are 2.2(2) and 108(14) mg h^{-1}, respectively. Parentheses contain 2σ uncertainties in the last significant digits.

IAP works by capturing a certain fraction of particles from the air passing through the purifier. The particle capture probability, γ, is related to the first-order particle removal rate constant, k_{ap}, the mass flow rate through the air purifier, F, and room volume, V, as follows:

$$k_{ap} = \gamma F/V \quad (1)$$

The γF product, which is related to the clean air delivery rate (CADR) of the air purifier, can be used to predict the effective particle removal rate constant in a well-mixed room of an arbitrary volume. The measured value of γF (see Supporting Information) is 342(20) SLM = 20(1) m^3 h^{-1} for the IAP. This value of γF was measured for particles that were predominantly in the 0.15−0.30 μm size range. This work assumes that the γF value is the same for all particle sizes of interest. It is certainly possible that IAP has different efficiencies for ultrafine and course particles (*47*), but this is not going to strongly affect the main conclusions of this work. OG was found to have no measurable effect on the particle count ($\gamma F \approx 0$) because it has no built-in particle filtration capabilities.

The actual tests were performed in a sparingly furnished office room with a floor area of 11.1 m^2 and overall volume of 27.1 m^3. The floor material was linoleum, the walls were

* Corresponding author phone: (949) 824-1262; fax: (949) 824-2420; e-mail: http://aerosol.chem.uci.edu/.

10.1021/es061760y CCC: $37.00
Published on Web 02/21/2007

TABLE 1. Parameters of Commercial IAP and OG Used in the Tests[a]

	IAP	OG
purchase date	2004	2004
model	SI637	Crystal Air Pro 420
O_3 emission rate (mg/h) ($\pm 2\sigma$)	2.2 ± 0.2	108 ± 14
clean air delivery rate, γF ($m^3\ h^{-1}$)	20 ± 1	0

[a] Measurements of ozone emission rates and particle removal rates are described in the Supporting Information.

painted drywall, and the ceiling consisted of industrial fiberglass ceiling tiles. The room was ventilated through an HVAC system with a measured whole air exchange rate of $\sim 5\ h^{-1}$. This exchange rate is higher than for an average private residence but typical for an office room. The air purifiers were positioned on the floor in the middle of the room. The ozone monitor and particle counters were installed in an adjacent room and air was sampled approximately 1 m away from the air purifiers.

A scanning mobility particle sizer (SMPS) was used to measure the particle size distribution in the 0.010−0.90 μm size range, and a laser particle counter sampled particles in the 0.15−5.0 μm size range. A large fan was placed in the room for a better mixing of the air across the room volume. The time to acquire one particle size distribution with SMPS was 7 min and that for laser particle counter was 5 min. In a typical run, the data were logged with a Labview-based program for 5−20 h with the air purifier turned off and then for another 5−20 h with the air purifier turned on. At certain time intervals, a measured quantity of D-limonene vapor (5−60 mg) was injected in the room at a rate of 3 mg min^{-1} for a brief period of time.

Kinetic Model. The following model is used to describe concentrations in a single well-mixed indoor environment that exchanges air with the exterior atmosphere:

$$\frac{d[X]}{dt} = \kappa_X \lambda [X]_{out} + \frac{E_X(t)}{V} + R_X - \lambda [X] - k_{rX}[X] - \frac{S}{V} v_{dX}[X] \quad (2)$$

[X] and $[X]_{out}$ are concentrations of species X indoors and outdoors, respectively; λ is the whole air exchange rate; κ_X is outdoor-to-indoor penetration efficiency; V is the volume; S is the interior surface area; E_X is the emission rate for X by all indoor sources; R_X is the combined rate of production of X by gas-phase chemistry; k_{rX} is an effective first-order rate constant for the removal of X by chemical reactions; v_{dX} is the deposition velocity of X on indoor surfaces. The constants λ, k_{rX}, and $k_{dX} = S/V\, v_{dX}$ all have units of inverse time, κ_X is unitless, and [X] has mass concentration units ($\mu g\ m^{-3}$) to simplify comparison of concentrations of gas-phase and aerosolized species.

Three species are included in the model: ozone, an unsaturated VOC (D-limonene), and PM. Ozone is emitted indoors by the air purifier and also penetrates from outdoors by means of air exchange. Aerosol particles are brought indoors by the HVAC system, and also chemically generated via reaction

$$VOC + O_3 \rightarrow \chi PM + \text{volatile organics} \quad (3)$$

where χ is the mass yield of aerosol resulting from the ozonolysis of VOC. The model implicitly assumes that all involatile products of VOC oxidation by ozone quickly partition themselves in the particle phase. The aerosol particles are not differentiated by size or composition; reaction 3 is simply assumed to increase the total mass concentration of PM in the room volume.

With these assumptions, the time evolution of ozone, reactive VOC, and aerosol concentrations can be written as follows.

$$\frac{d[O_3]}{dt} = \lambda \kappa_{O_3}[O_3]_{out} + \frac{E_{O_3}}{V} - (\lambda + k_{dO_3} + k_r[VOC])[O_3] \quad (4)$$

$$\frac{d[VOC]}{dt} = \lambda \kappa_{VOC}[VOC]_{out} + \frac{E_{VOC}}{V} - (\lambda + k_{dVOC} + k_r[O_3])[VOC] \quad (5)$$

$$\frac{d[PM]}{dt} = \lambda \kappa_{PM}[PM]_{out} + \chi k_r[VOC][O_3] - (\lambda + k_{dPM} + k_{ap})[PM] \quad (6)$$

In the last equation, we separated the removal of aerosol particles by wall deposition (k_{dPM}) and by the air purifier (k_{ap}). The latter can be calculated from eq 1. These equations will be used below to simulate the indoor VOC, PM, and ozone concentrations either analytically or numerically.

Results

Steady-State Kinetic Model. In the experiments and simulations described here, and also in many realistic indoor environments, the ozone removal is often dominated by either air exchange or surface deposition. Gas-phase reactions normally make a much smaller contribution to the ozone removal rate. Under such conditions, the term $k_r[VOC]$ in eq 4 can be neglected compared to λ and k_{dO_3}. With this simplifying assumption, the equations can be easily solved in steady-state (ss) for the case of time-independent emission rates E_{O_3} and E_{VOC}. The steady-state concentration of ozone depends on whether the air purifier is turned on or off:

$$[O_3]_{ss}^{ON} \cong \frac{E_{O_3}/V + \lambda \kappa_{O_3}[O_3]_{out}}{\lambda + k_{dO_3}} \quad (7)$$

$$[O_3]_{ss}^{OFF} \cong \frac{\lambda \kappa_{O_3}[O_3]_{out}}{\lambda + k_{dO_3}} \quad (8)$$

This dependence propagates into the steady-state concentrations of VOC and aerosol particles.

$$[VOC]_{ss}^{ON/OFF} \cong \frac{\lambda \kappa_{VOC}[VOC]_{out} + E_{VOC}/V}{\lambda + k_{dVOC} + k_r[O_3]_{ss}^{ON/OFF}} \quad (9)$$

$$[PM]_{ss}^{ON/OFF} = \frac{\lambda \kappa_{PM}[PM]_{out} + \chi k_r[O_3]_{ss}^{ON/OFF}[VOC]_{ss}^{ON/OFF}}{\lambda + k_{dPM} + k_{ap}} \quad (10)$$

The time it takes for the concentrations to approach their steady-state values is inversely proportional to the corresponding removal rates, i.e., values in the denominators of eqs 8−10. For the base conditions listed in Table 2, these times are 0.3, 1.4, and 2 h for ozone, particles, and VOC, respectively.

To quantify the effect of the air purifier on particle concentration in the room, we define an efficiency parameter K, as the ratio of the steady-state PM concentrations obtained when the air purifier is turned on to that when it is off.

$$K = \frac{[PM]_{ss}^{ON}}{[PM]_{ss}^{OFF}} = \frac{\lambda + k_{dPM}}{\lambda + k_{dPM} + k_{ap}} \times \frac{\lambda \kappa_{PM}[PM]_{out} + \chi k_r[O_3]_{ss}^{ON}[VOC]_{ss}^{ON}}{\lambda \kappa_{PM}[PM]_{out} + \chi k_r[O_3]_{ss}^{OFF}[VOC]_{ss}^{OFF}} \quad (11)$$

TABLE 2. Kinetic Model Parameters[a]

parameter	definition	base values for calculation of K	values for simulation of particle bursts
V	room volume	50 m^3	27.1 m^3 (measured)
$[O_3]_{out}$	outside ozone	30 ppb	5 ppb (measured)
$[PM]_{out}$	outside PM	10 $\mu g\ m^{-3}$	0.55 $\mu g\ m^{-3}$ ($[PM_{0.12}]$)
$[VOC]_{out}$	outside VOC	0.0 $\mu g\ m^{-3}$	0.0 $\mu g\ m^{-3}$ (assumed)
λ	air exchange rate	0.5 h^{-1}	5.0 h^{-1} (measured)
k_{dO_3}	ozone surface deposition	2.8 h^{-1}	1.0 h^{-1} (estimated)
k_{dPM}	PM surface deposition	0.2 h^{-1}	0.2 h^{-1} (assumed)
k_{dVOC}	VOC surface deposition	0.0 h^{-1}	0.0 h^{-1} (assumed)
k_r	VOC + O_3 rate constant	2.0×10^{-16} $cm^3\ s^{-1}$	2.0×10^{-16} $cm^3\ s^{-1}$
χ	aerosol mass yield	1.0	0.13 (fitted)
κ_X	all penetration efficiencies	1.0	1.0 (assumed)
E_{VOC}	VOC indoor emission rate	5 mg h^{-1}	5 min pulse at 3 mg h^{-1}
E_{O_3}	ozone indoor emission rate	variable 0−10 mg h^{-1}	2.2 mg h^{-1} (SI637)
γF	clean air delivery rate	variable 0−100 $m^3\ h^{-1}$	20 $m^3\ h^{-1}$ (SI637)

[a]The third column lists the base parameters used for steady-state calculation of the air purifier efficiency, K, from eq 11. The forth column lists parameters used in the simulation of particle bursts observed in the office room with operating IAP. $[PM]_{out}$ refers to the $[PM_{all\ sizes}]$ and $[PM_{0.12}]$ in columns 3 and 4, respectively.

Operation of an effective air purifier should result in conditions corresponding to $K << 1$. When $K > 1$, the device actually makes more particles than it removes, thus acting as a net particle emitter. The situation with $K = 1$ corresponds to the exact cancellation of the particle removal and generation rates.

The first term in this equation describes the effect of the air purifier in the absence of any indoor chemistry.

$$K_{base} = \left(1 + \frac{k_{ap}}{\lambda + k_{dPM}}\right)^{-1} \quad (12)$$

The more effective the air purifier the smaller is the values of K_{base}. It is close to unity for an ineffective air purifier ($k_{ap} \ll \lambda + k_{dPM}$). A similar parameter was used to characterize air cleaners in ref *48*.

The second term in eq 11 corresponds to the effect of indoor particle generation from the VOC oxidation by ozone. It is unity for air purifiers that emit no ozone or for rooms containing negligible amounts of reactive VOC, but it can be substantially larger than unity if both ozone and reactive VOC are present. In such cases, the effect of indoor chemistry can make the overall value of $K > 1$ (air contamination) even if $K_{base} < 1$.

We have calculated values of K for a typical indoor environment as a function of the ozone emission rate and clean air delivery rate from the air purifier (γF). Table 2 lists the calculation parameters. The outside ozone, PM, and unsaturated VOC concentrations are 30 ppb, 10 $\mu g/m^3$, and 0 $\mu g/m^3$, respectively, characteristic of reasonably clean air. The whole air exchange rate $\lambda = 0.5\ h^{-1}$ comes from an analysis of multiple residences (*49*, *50*). The value $k_{dO_3} = 2.8\ h^{-1}$ is adopted for a typical surface removal rate constant for ozone (*44*, *51*). The corresponding rate constant for particles is $k_{dPM} = 0.2\ h^{-1}$, a value suitable for a sparsely furnished room (*49*, *52*). It is known that particle deposition rates depend on particle size (*47*, *52*), but this dependence is not explicitly considered in this model in order to keep it simple. All penetration efficiencies are set to $\kappa = 1$ (setting them to smaller values would only make the predicted K higher).

The VOC emission rate is assumed to be $E_{VOC} = 5$ mg/h (this corresponds to the evaporation of 0.5 g of a cleaning solution containing 1% limonene in 1 h). This value is comparable to the combined emission rate of aerosol-forming terpenes in realistic indoor environments (*28*, *42*). The rate constant for the reaction between VOC and ozone corresponds to that for limonene (*12*). The aerosol mass yield is difficult to estimate as it depends in a complicated way on the preexisting PM concentration, concentrations of reactants, and many other factors. This model assumes that $\chi = 1$, but we also show results for a 1 order of magnitude reduction in the yield. Surface deposition of VOC is neglected. The ozone emission rate is varied over the range expected for a typical ionization air purifier, 0−10 mg/h (*34*).

Figure 1 shows the calculated $K = 1$ curves for several different scenarios. Everything above the $K = 1$ curves corresponds to $K < 1$ (air purification) and everything below the curves corresponds to $K > 1$ (air contamination). In addition to the base conditions listed in Table 2, Figure 1 also presents calculations for $[O_3]_{out}$, $[PM]_{out}$, or air exchange rate, λ, scaled by 1 order of magnitude. Although it is not directly obvious from eq 11, an increase in $[PM]_{out}$ by a certain factor is exactly equivalent to a decrease in the VOC emission rate, E_{VOC}, or to a decrease in the aerosol mass yield, χ, by the same factor. For example, the bottom curve in panel b is equivalent to the base conditions with χ changed to 0.1, a more realistic SOA yield for low concentrations of reactants (*53*).

Ozone-free air purifiers fall on the vertical axes ($E_{O_3} = 0$) in Figure 1. They are always characterized by $K \leq 1$ as predicted by eq 12. Pure ozone generators fall on the horizontal axes ($\gamma F = 0$), and always have $K \geq 1$. The ionization air purifiers that both remove particles and emit ozone represent the most interesting case. For example, the IAP used here ($\gamma F = 20(1)\ m^3\ h^{-1}$ and $E_{O_3} = 2.2(2)$ mg h^{-1}) falls slightly below the $K = 1$ curve for the base-case scenario. With the predicted value of $K = 1.12$, this device would not act as a purifier under the base conditions listed in Table 2. Decreasing the outside concentrations of PM or ozone, decreasing the air exchange rate, or increasing the indoor VOC emission rate would make the situation even worse.

Indoor SOA Nucleation Events. Aerosol particle generation was tested for both IAP and OG in a 27.1 m^3 office room. Figure 2 shows a sample data run. Operation of OG normally increased the ozone steady-state concentration by some 250 ppb above the 5 ppb background. Operation of IAP increased it by ~5−15 ppb above the background, in rough proportion to its ozone emission rate (*34*). The triangles in Figure 2 indicate the time when a certain amount (5−60 mg) of limonene vapor was injected into the room.

Continuous operation of IAP in the absence of limonene resulted in a slight (<20%) reduction in the average particle concentration. For the 27.1-m^3 room volume, the expected particle removal rate constant by IAP is $k_{ap} = 0.76\ h^{-1}$. The measured air exchange rate for this room is $\lambda \sim 5\ h^{-1}$. Neglecting the particle wall deposition, eq 12 predicts 10−

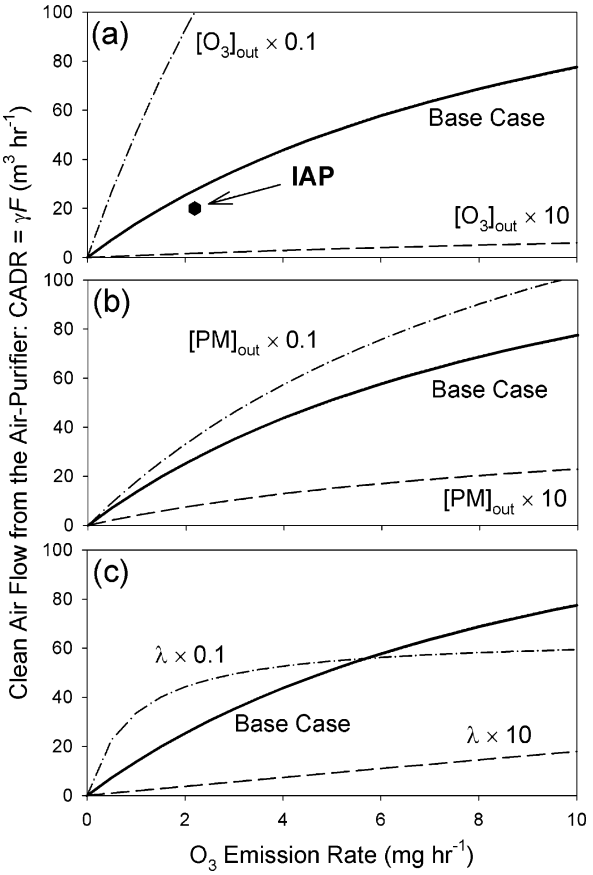

FIGURE 1. Conditions resulting in an exact cancellation of particle generation and removal by ozone-emitting air purifiers. Solid lines are $K = 1$ curves for the base conditions listed in Table 2. Areas above and below the $K = 1$ curves correspond to air purification ($K < 1$) and contamination ($K > 1$), respectively. Panels a−c display $K = 1$ curves for 10-fold deviations from the base conditions in $[O_3]_{out}$, $[PM]_{out}$, and λ, respectively. An increase in $[PM]_{out}$ is exactly equivalent to a decrease in E_{VOC} or χ by the same factor. Panel a includes the parameters of the IAP used in this work.

15% reduction in the particle count, in agreement with our observations. As expected, operation of OG had no detectable effect on the particle concentration.

Injections of limonene into the room during operation of either OG (injections 1−4 in Figure 2) or IAP (injections 5 and 6) reproducibly increased the particle number concentration by 1−2 orders of magnitude. On the contrary, injections of limonene without operating air purifiers (e.g., injection 7 in Figure 2) produced little change in the particle concentration; a small increase was observed only in 10−15% of such injections. Very infrequently, a spontaneous increase in the particle number concentration would occur (Figure 2). These spontaneous bursts were of an external origin and penetrated into the room through the HVAC system.

The limonene injection rate (3 mg min^{-1}) was higher than one could expect for a typical indoor source. However, the injection lasted only a short time, and the total mass of injected limonene was comparable to what one could get from a room cleaning using a limonene-containing cleaning solution (*27*).

Steady-state ozone concentration decreased at most 10−20% for a short period of time following the injection. (The spikes in $[O_3]$ in Figure 2 are artifacts resulting from the contribution of particles to the overall UV absorption sensed by the ozone monitor.) This small effect on the ozone concentration is due to the relatively small rate of reaction

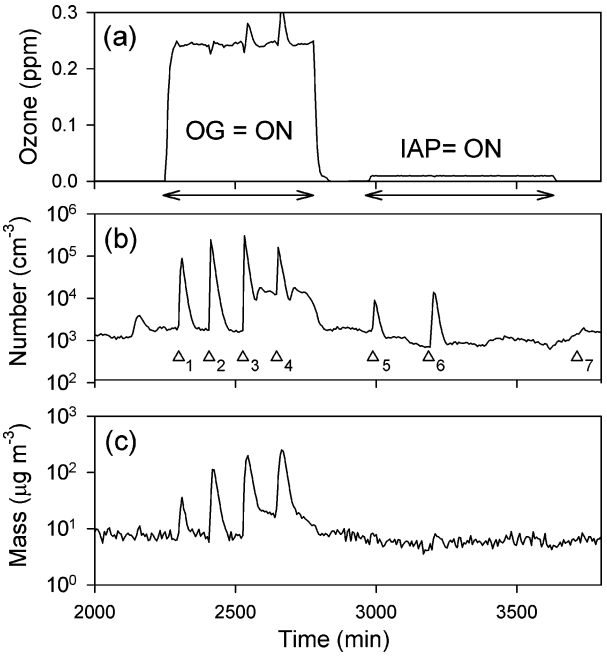

FIGURE 2. Sample measurements of ozone (a) and particle (b) concentrations in a ventilated office. Two plateaus in $[O_3]$ correspond to the OG and IAP operation. Spikes in $[O_3]$ are experimental artifacts (see text). Panels b and c display the total number and mass concentrations of particles in the 0.01−0.9 μm size range. Triangles represent injections of limonene in the room at a rate of 3 mg min^{-1}; injections 1−7 lasted 5, 10, 15, 20, 5, 15, and 15 min, respectively.

(*3*). Indeed, an instantaneous 10-mg limonene injection into the 27.1-m^3 room volume would correspond to the initial concentration of 1.6×10^{12} molecules/cm^{-3}. Even at this high concentration, the VOC + O_3 reaction's contribution to the ozone removal rate is only 1.2 h^{-1}. The air exchange rate, $\lambda \approx 5$ h^{-1}, and ozone deposition rate, $k_{dO_3} = 2.8$ h^{-1} (*44*, *51*) are considerably higher. The effect of VOC on the ozone concentration is expected to be even smaller if VOC are emitted over an extended period of time. The same arguments were used to justify neglecting the k_r[VOC] term in eq 4 in the steady-state model described above.

Figure 2c shows the total particle mass concentration computed from the particle size distribution assuming spherical particles with a density of 1 g/cm^3. While limonene injections 1−4 occurring at $[O_3]_{ss} = 250$ ppb produce clear peaks in the total particle mass concentration, injections 5 and 6 occurring at 10−15 ppb ozone increase the number but not the total mass of the particles. This is a clear indication that the limonene oxidation products not only condense onto pre-existing particles but also nucleate homogeneously. A similar conclusion was reached in a chamber study of ozone reacting with selected household products (*28*). The resulting new particles are in the ultrafine size domain (~0.1 μm), and therefore do not significantly contribute to the total mass.

Figure 3 shows a filled contour plot of two particle bursts corresponding to injections 1 and 2 in Figure 2. In the first case, corresponding to the addition of 15 mg of limonene over 5 min, the particle size distribution peaks below 0.1 μm. In the second case, corresponding to the addition of 30 mg of limonene over 10 min, the resulting particle size distribution is bimodal, reflecting complicated particle nucleation and growth dynamics. The structure of these particle bursts bears a resemblance to the particle nucleation events frequently observed outdoors (*54*−*56*). The main difference is that the size distribution evolves considerably faster under the present conditions of large concentrations of reactants and fast air exchange rates.

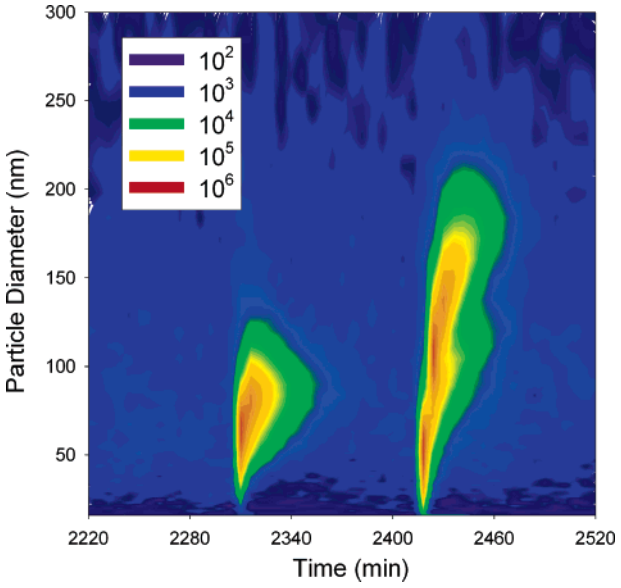

FIGURE 3. Contour plot of particle bursts caused by addition of limonene to the office room with an operating OG (injections 1 and 2 in Figure 2). The color contours correspond to the particle size distribution, d*N*/d log *D*, in units of cm^{-3}, logarithmically distributed.

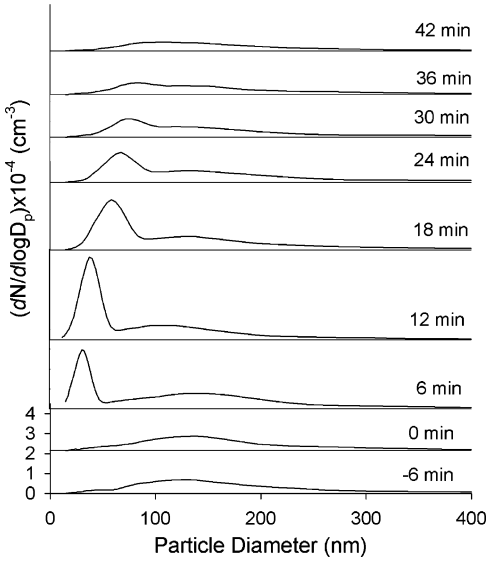

FIGURE 4. Particle size distributions observed after adding limonene to the office room with an operating IAP. Each distribution takes 6 min to acquire; limonene is injected in the middle of the "0 min" scan. The distributions are offset for clarity. The vertical scales on all plots are identical; the tick labels are shown for the "-6 min" plot only.

Figure 4 displays the time evolution in the particle size distribution resulting from an addition of 15 mg of limonene in 5 min into the room with IAP turned on. Each size distribution took 6 min to acquire, with SMPS scanning in the direction of increasing particle diameter. New particles appear immediately after the limonene addition. They grow from their initial diameter of 0.02−0.03 μm to ~0.08−0.1 μm before being driven out of the room by the HVAC air flow.

Model Evaluation. The observed particle bursts were fitted to the kinetic model described above in one of the following ways. The first approach was a numeric solution of eqs 4−6 using a stiff differential equation solver. The injection of limonene was treated as a 3 mg min^{-1} limonene source turned on for a certain period of time. The second approach was an analytical solution of eqs 4−6, under the simplifying assumptions of an instantaneous jump in VOC concentration by the amount of $[VOC]_{added}$ (i.e., the amount that is added over the entire injection period) and a constant ozone concentration in the room. Once again, the second assumption means that $[O_3]_{ss}$ is not strongly affected by the presence of limonene. The resulting solutions are

$$[VOC](t) = [VOC]_{ss}^{ON} + [VOC]_{added} e^{-k_{VOC}t} \quad (13)$$

$$[PM](t) = [PM]_{ss}^{ON} + \frac{\chi k_r [VOC]_{added} [O_3]_{ss}^{ON}}{k_{PM} - k_{VOC}} (e^{-k_{VOC}t} - e^{-k_{PM}t}) \quad (14)$$

k_{VOC} and k_{PM} are the effective rate constants for the removal of VOC and PM, respectively,

$$k_{VOC} = \lambda + k_{dVOC} + k_r [O_3]_{ss}^{ON} \quad (15)$$

$$k_{PM} = \lambda + k_{dPM} + k_{ap} \quad (16)$$

The initial steady-state concentrations are calculated from eqs 7−10.

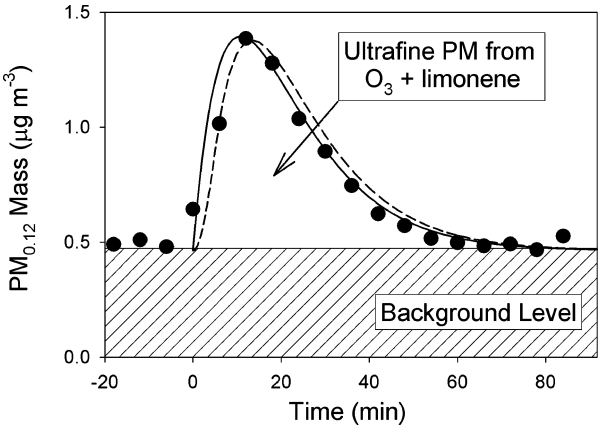

FIGURE 5. Simulations of a representative particle burst event resulting from an addition of 15 mg of limonene (for 5 min at t = 0) to the office room with operating IAP. Dots: experimental total particle mass concentration for particles with diameters below 0.12 μm ($PM_{0.12}$). Solid line: approximate analytical solution calculated from eq 14. Dashed line: exact numeric simulation of eqs 4−6.

Figure 5 shows the results of the simulations. The experimental data points represent the total mass concentration of particles following an injection of 15 mg of limonene over 5 min into the room with an operating IAP. Because the particles are small, the total mass is calculated only for particles below 0.12 μm in diameter under the usual assumptions of particles' sphericity and unit density. The simulation parameters (Table 2) are explicitly measured, estimated, or taken from the literature. For example, the outdoor particle concentration, $[PM_{0.12}]_{out} = 0.55$ μg m^{-3}, is chosen to match the background particle mass concentration for particles with $D_p < 0.12$ μm for that particular measurement. The only adjustable parameter in the fit is the mass yield of aerosol particles, χ.

Figure 5 shows that both exact and approximate simulations provide a satisfactory fit to the data. The fitted mass yield of aerosol particles is $\chi = 0.13$ for this particular measurement. The fitted yield becomes higher for elevated $[O_3]_{ss}$ or larger amounts of injected limonene. This explains why the particle bursts resulting from injections 1−4 in Figure 2 are stronger than the ones from injections 5 and 6. These results are in qualitative agreement with published chamber

studies of SOA yields, which find that the yields increase with the concentration of both VOC and O_3 (*15*, *53*, *57*, *58*).

Discussion

Concerns about ozone-emitting air purifiers have been and continue to be raised by scientists and government officials (*32*, *34*, *35*, *44*, *59*). Thus, in a recent report to the California Legislature, the California Air Resources Board officially recommended that the public avoid using these devices indoors (*33*). This important report reviewed both direct and indirect health effects of the artificially elevated indoor ozone concentrations.

This paper evaluates a simple kinetic model that can be used to quantify the indirect effect of ozone−VOC chemistry on the level of indoor PM. This model includes only three chemical species, but it grasps all the key elements of the ozone−VOC chemistry. It should be directly applicable under conditions when the reactive VOC emissions are dominated by one molecule or by several molecules with comparable reactivities toward ozone. In more complicated VOC emission scenarios, the model can be expanded to include multiple SOA-forming reactions between ozone and VOC.

The most striking prediction of the model is the small magnitude of the air purifier's ozone emission rate needed to significantly increase the PM level in the air under realistic indoor conditions. Indeed, under the base conditions listed in Table 2, an air purifier with $E_{O_3}/\gamma F$ ratio exceeding ~0.1 mg m^{-3} (i.e., 0.1 mg of ozone emitted into every cubic meter of air processed by the air purifier) may *increase* the respirable PM mass concentration instead of reducing it as advertised by the manufacturer. It is also of concern that this condition is actually fulfilled by IAP used in this work: an appliance that had a broad commercial availability as recently as 2005. Reduction of the ozone emission rate (ideally to zero level) and increasing the air flow through the air purifier are the most important factors for achieving the maximum possible reduction in the indoor PM level. Operation of ozone-emitting air purifiers in indoor environments with elevated concentrations of unsaturated VOC should be avoided.

Acknowledgments

This study was supported by the National Science Foundation through Environmental Molecular Science Institute program, grant CHE-0431312 (formerly CHE-0209719), and Atmospheric Chemistry Program, grant ATM-0509248. The authors thank Dr. James Pitts Jr. for stimulating discussions.

Supporting Information Available

Supporting information describes characterization of the ozone emission rates and particle removal rates for the two air purifiers used in this study.

Literature Cited

(1) Pope, C. A., III. Review: epidemiological basis for particulate air pollution health standards. *Aerosol. Sci. Technol.* **2000**, *32*, 4−14.

(2) Gauderman, W. J.; Gilliland, G. F.; Vora, H.; Avol, E.; Stram, D.; McConnell, R.; Thomas, D.; Lurmann, F.; Margolis, Helene, G.; Rappaport Edward, B.; Berhane, K.; Peters, John, M. Association between air pollution and lung function growth in southern California children: results from a second cohort. *Am. J. Respir. Crit. Care Med.* **2000**, *166*, 76−84.

(3) von Klot, S.; Woelke, G.; Tuch, T.; Heinrich, J.; Dockery, D. W.; Schwartz, J.; Kreyling, W. G.; Wichmann, H. E.; Peters, A. Increased asthma medication use in association with ambient fine and ultrafine particles. *Eur. Respir. J.* **2002**, *20*, 691−702.

(4) Delfino, R. J.; Zeiger, R. S.; Seltzer, J. M.; Street, D. H.; McLaren, C. E. Association of asthma symptoms with peak particulate air pollution and effect modification by anti-inflammatory medication use. *Environ. Health Perspect.* **2002**, *110*, A607−A617.

(5) Von Klot, S.; Peters, A.; Aalto, P.; Bellander, T.; Berglind, N.; D'Ippoliti, D.; Elosua, R.; Hoermann, A.; Kulmala, M.; Lanki, T.; Loewel, H.; Pekkanen, J.; Picciotto, S.; Sunyer, J.; Forastiere, F. Ambient air pollution is associated with increased risk of hospital cardiac readmissions of myocardial infarction survivors in five European cities. *Circulation* **2005**, *112*, 3073−3079.

(6) Schulz, H.; Harder, V.; Ibald-Mulli, A.; Khandoga, A.; Koenig, W.; Krombach, F.; Radykewicz, R.; Stampfl, A.; Thorand, B.; Peters, A. Cardiovascular effects of fine and ultrafine particles. *J. Aerosol Med.* **2005**, *18*, 1−22.

(7) Dockery, D. W.; Pope, C. A., 3rd; Xu, X.; Spengler, J. D.; Ware, J. H.; Fay, M. E.; Ferris, B. G., Jr.; Speizer, F. E. An association between air pollution and mortality in six U.S. cities. *New Engl. J. Med.* **1993**, *329*, 1753−1759.

(8) Pope, C. A., III; Burnett, R. T.; Thun, M. J.; Calle, E. E.; Krewski, D.; Ito, K.; Thurston, G. D. Lung cancer, cardiopulmonary mortality, and long-term exposure to fine particulate air pollution. *J. Am. Med. Assoc.* **2002**, *287*, 1132−1141.

(9) Cohen, A. J.; Pope, C. A., 3rd. Lung cancer and air pollution. *Environ. Health Perspect.* **1995**, *103*, 219−224.

(10) Krewski, D.; Burnett, R.; Jerrett, M.; Pope, C. A.; Rainham, D.; Calle, E.; Thurston, G.; Thun, M. Mortality and long-term exposure to ambient air pollution: ongoing analyses based on the American cancer society cohort. *J. Toxicol. Environ. Health, Part A* **2005**, *68*, 1093−1109.

(11) Oberdoerster, G.; Sharp, Z.; Atudorei, V.; Elder, A.; Gelein, R.; Kreyling, W.; Cox, C. Translocation of inhaled ultrafine particles to the brain. *Inhalation Toxicol.* **2004**, *16*, 437−445.

(12) Finlayson-Pitts, B. J.; Pitts, J. N. *Chemistry of the Upper and Lower Atmosphere: Theory, Experiments, and Applications*; Academic Press: New York, 2000.

(13) Sarwar, G.; Olson, D. A.; Corsi, R. L.; Weschler, C. J. Indoor fine particles: the role of terpene emissions from consumer products. *JAWMA* **2004**, *54*, 367−377.

(14) Weschler, C. J.; Shields, H. C. Indoor ozone/terpene reactions as a source of indoor particles. *Atmos. Environ.* **1999**, *33*, 2301−2312.

(15) Odum, J. R.; Hoffmann, T.; Bowman, F.; Collins, D.; Flagan, R. C.; Seinfeld, J. H. Gas/particle partitioning and secondary organic aerosol yields. *Environ. Sci. Technol.* **1996**, *30*, 2580−2585.

(16) Hoffmann, T.; Odum, J. R.; Bowman, F.; Collins, D.; Klockow, D.; Flagan, R. C.; Seinfeld, J. H. Formation of organic aerosols from the oxidation of biogenic hydrocarbons. *J. Atmos. Chem.* **1997**, *26*, 189−222.

(17) Sax, M.; Zenobi, R.; Baltensperger, U.; Kalberer, M. Time resolved infrared spectroscopic analysis of aerosol formed by photo-oxidation of 1,3,5-trimethylbenzene and α-pinene. *Aerosol Sci. Technol.* **2005**, *39*, 822−830.

(18) Koch, S.; Winterhalter, R.; Uherek, E.; Kolloff, A.; Neeb, P.; Moortgat, G. K. Formation of new particles in the gas-phase ozonolysis of monoterpenes. *Atmos. Environ.* **2000**, *34*, 4031−4042.

(19) Bonn, B.; Schuster, G.; Moortgat, G. K. Influence of water vapor on the process of new particle formation during monoterpene ozonolysis. *J. Phys. Chem. A* **2002**, *106*, 2869−2881.

(20) Czoschke, N. M.; Jang, M.; Kamens, R. M. Effect of acidic seed on biogenic secondary organic aerosol growth. *Atmos. Environ.* **2003**, *37*, 4287−4299.

(21) Gao, S.; Keywood, M.; Ng, N. L.; Surratt, J.; Varutbangkul, V.; Bahreini, R.; Flagan, R. C.; Seinfeld, J. H. Low-molecular-weight and oligomeric components in secondary organic aerosol from the ozonolysis of cycloalkenes and α-pinene. *J. Phys. Chem. A* **2004**, *108*, 10147−10164.

(22) Iinuma, Y.; Boge, O.; Gnauk, T.; Herrmann, H. Aerosol-chamber study of the α-pinene/O_3 reaction: influence of particle acidity on aerosol yields and products. *Atmos. Environ.*. **2004**, *38*, 761−773.

(23) Baltensperger, U.; Kalberer, M.; Dommen, J.; Paulsen, D.; Alfarra, M. R.; Coe, H.; Fisseha, R.; Gascho, A.; Gysel, M.; Nyeki, S.; Sax, M.; Steinbacher, M.; Prevot, A. S. H.; Sjogren, S.; Weingartner, E.; Zenobi, R. Secondary organic aerosols from anthropogenic and biogenic precursors. *Faraday Discuss.* **2005**, *130*, 265−278.

(24) Bahreini, R.; Keywood, M. D.; Ng, N. L.; Varutbangkul, V.; Gao, S.; Flagan, R. C.; Seinfeld, J. H.; Worsnop, D. R.; Jimenez, J. L. Measurements of secondary organic aerosol from oxidation of cycloalkenes, terpenes, and *m*-xylene using an aerodyne aerosol mass spectrometer. *Environ. Sci. Technol.* **2005**, *39*, 5674−5688.

(25) Tolocka, M. P.; Jang, M.; Ginter, J. M.; Cox, F. J.; Kamens, R. M.; Johnston, M. V. Formation of oligomers in secondary organic aerosol. *Environ. Sci. Technol.* **2004**, *38*, 1428−1434.

(26) Presto, A. A.; Huff Hartz, K. E.; Donahue, N. M. Secondary organic aerosol production from terpene ozonolysis. 2. Effect of NO_x concentration. *Environ. Sci. Technol.* **2005**, *39*, 7046−7054.

(27) Singer, B. C.; Coleman, B. K.; Destaillats, H.; Hodgson, A. T.; Lunden, M. M.; Weschler, C. J.; Nazaroff, W. W. Indoor secondary pollutants from cleaning product and air freshener use in the presence of ozone. *Atmos. Environ.* **2006**, *40*, 6696−6710.
(28) Destaillats, H.; Lunden, M. M.; Singer, B. C.; Coleman, B. K.; Hodgson, A. T.; Weschler, C. J.; Nazaroff, W. W. Indoor secondary pollutants from household product emissions in the presence of ozone: a bench-scale chamber study. *Environ. Sci. Technol.* **2006**, *40*, 4421−4428.
(29) Rohr, A. C.; Weschler, C. J.; Koutrakis, P.; Spengler, J. D. Generation and quantification of ultrafine particles through terpene/ozone reaction in a chamber setting. *Aerosol Sci. Technol.* **2003**, *37*, 65−78.
(30) Liu, X.; Mason, M.; Krebs, K.; Sparks, L. Full-scale chamber investigation and simulation of air freshener emissions in the presence of ozone. *Environ. Sci. Technol.* **2004**, *38*, 2802−2812.
(31) Wainman, T.; Zhang, J.; Weschler, C. J.; Lioy, P. J. Ozone and limonene in indoor air: a source of submicron particle exposure. *Environ. Health Perspect.* **2000**, *108*, 1139−1145.
(32) Phillips, T.; Jakober, C. Evaluation of ozone emissions from portable indoor "air cleaners" that intentionally generate ozone California Air Resources Board, 2006.
(33) Indoor air pollution in California: AB1173 report to the California legislature, California Air Resources Board, 2005.
(34) Britigan, N.; Alshawa, A.; Nizkorodov, S. A. Quantification of ozone levels in indoor environments generated by ionic and ozonolysis air purifiers. *JAWMA* **2006**, *56*, 601−610.
(35) Phillips, T. J.; Bloudoff, D. P.; Jenkins, P. L.; Stroud, K. R. Ozone emissions from a "personal air purifier". *J. Exposure Anal. Environ. Epidemiol.* **1999**, *9*, 594−601.
(36) *WHO air quality guidelines for Europe*, 2nd ed.; WHO Regional Publications, European Series, No. 91; 2000.
(37) Moriske, H.-J.; Ebert, G.; Konieczny, L.; Menk, G. Concentrations and decay rates of ozone in indoor air in dependence on building and surface materials. *Toxicol. Lett.* **1998**, *96/97*, 319−323.
(38) Grontoft, T.; Raychaudhuri, M. R. Compilation of tables of surface deposition velocities for O_3, NO_2 and SO_2 to a range of indoor surfaces. *Atmos. Environ.* **2004**, *38*, 533−544.
(39) Sabersky, R. H.; Sinema, D. A.; Shair, F. H. Concentrations, decay rates, and removal of ozone and their relation to establishing clean indoor air. *Environ. Sci. Technol.* **1973**, *7*, 347−353.
(40) Morrison, G. C.; Nazaroff, W. W. Ozone interactions with carpet: secondary emissions of aldehydes. *Environ. Sci. Technol.* **2002**, *36*, 2185−2192.
(41) Knudsen, H. N.; Nielsen, P. A.; Clausen, P. A.; Wilkins, C. K.; Wolkoff, P. Sensory evaluation of emissions from selected building products exposed to ozone. *Indoor Air* **2003**, *13*, 223−231.
(42) Sarwar, G.; Corsi, R.; Kimura, Y.; Allen, D.; Weschler, C. J. Hydroxyl radicals in indoor environments. *Atmos. Environ.* **2002**, *36*, 3973−3988.
(43) Weschler, C. J. Indoor chemistry as a source of particles. In *Indoor environment: Airborne particles and settled dust*; Morawska, L., Salthammer, T., Eds.; Wiley-VCH: Weinheim, Germany, 2003; pp 171−194.
(44) Weschler, C. J. Ozone in indoor environments: Concentration and chemistry. *Indoor Air* **2000**, *10*, 269−288.
(45) Nojgaard, J. K.; Christensen, K. B.; Wolkoff, P. The effect on human eye blink frequency of exposure to limonene oxidation products and methacrolein. *Toxicol. Lett.* **2005**, *156*, 241−251.
(46) Wolkoff, P.; Clausen, P. A.; Wilkins, C. K.; Nielsen, G. D. Formation of strong airway irritants in terpene/ozone mixtures. *Indoor Air* **2000**, *10*, 82−91.
(47) Lai, A. C. K.; Nazaroff, W. W. Modeling indoor particle deposition from turbulent flow onto smooth surfaces. *J. Aerosol Sci.* **2000**, *31*, 463−476.
(48) Ward, M.; Siegel, J. A.; Corsi, R. L. The effectiveness of stand alone air cleaners for shelter-in-place. *Indoor Air* **2005**, *15*, 127−134.
(49) Allen, R.; Larson, T.; Sheppard, L.; Wallace, L.; Liu, L. J. S. Use of real-time light scattering data to estimate the contribution of infiltrated and indoor-generated particles to indoor air. *Environ. Sci. Technol.* **2003**, *37*, 3484−3492.
(50) Wallace, L. Indoor particles: a review. *JAWMA* **1996**, *46*, 98−126.
(51) Lee, K.; Vallarino, J.; Dumyahn, T.; Ozkaynak, H.; Spengler, J. D. Ozone decay rates in residences. *JAWMA* **1999**, *49*, 1238−1244.
(52) Thatcher, T. L.; Lai, A. C. K.; Moreno-Jackson, R.; Sextro, R. G.; Nazaroff, W. W. Effects of room furnishings and air speed on particle deposition rates indoors. *Atmos. Environ.* **2002**, *36*, 1811−1819.
(53) Grosjean, D.; Williams, E. L., II; Grosjean, E.; Andino, J. M.; Seinfeld, J. H. Atmospheric oxidation of biogenic hydrocarbons: reaction of ozone with β-pinene, D-limonene, and *trans*-caryophyllene. *Environ. Sci. Technol.* **1993**, *27*, 2754−2758.
(54) Stanier, C. O.; Khlystov, A. Y.; Pandis, S. N. Nucleation events during the Pittsburgh air quality study: Description and relation to key meteorological, gas phase, and aerosol parameters. *Aerosol Sci. Technol.* **2004**, *38*, 253−264.
(55) Dunn, M. J.; Jimenez, J.-L.; Baumgardner, D.; Castro, T.; McMurry, P. H.; Smith, J. N. Measurements of Mexico City nanoparticle size distributions: Observations of new particle formation and growth. *Geophys. Res. Lett.* **2004**, *31*, L10102/10101-04.
(56) Tolocka, M. P.; Lake, D. A.; Johnston, M. V.; Wexler, A. S. Ultrafine nitrate particle events in Baltimore observed by real-time single particle mass spectrometry. *Atmos. Environ.* **2004**, *38*, 3215−3223.
(57) Kroll, J. H.; Ng, N. L.; Murphy, S. M.; Flagan, R. C.; Seinfeld, J. H. Secondary organic aerosol formation from isoprene photooxidation under high-NO_x conditions. *Geophys. Res. Lett.* **2005**, *32*, L18808/18801-04.
(58) Donahue, N. M.; Hartz, K. E. H.; Chuong, B.; Presto, A. A.; Stanier, C. O.; Rosenhorn, T.; Robinson, A. L.; Pandis, S. N. Critical factors determining the variation in SOA yields from terpene ozonolysis: A combined experimental and computational study. *Faraday Discuss.* **2005**, *130*, 295−309.
(59) Boeniger, M. F. Use of ozone generating devices to improve indoor air quality. *Am. Ind. Hyg. Assoc. J.* **1995**, *56*, 590−598.

Received for review July 24, 2006. Revised manuscript received October 23, 2006. Accepted January 19, 2007.

ES061760Y